Bank of Japan Working Paper Series

A Preferred Habitat View of Yield Curve Control

Junko Koeda *
jkoeda@waseda.jp

Yoichi Ueno **

No.22-E-7
August 2022

Bank of Japan
2-1-1 Nihonbashi-Hongokucho, Chuo-ku, Tokyo 103-0021, Japan

* Waseda University
**Monetary Affairs Department (currently Personnel and Corporate Affairs Department)

A Preferred Habitat View of Yield Curve Control*

Junko Koeda† and Yoichi Ueno‡

Abstract

We extend the canonical preferred habitat term structure model of Vayanos and Vila (2021) to analyze yield curve control (YCC) by treating the central bank as a preferred habitat investor allowing the price elasticity of government bond demand to depend on its targeted yield. The price elasticity captures the strictness of YCC implemented by the central bank. We calibrate the model for Japan and find that sufficiently strict YCC requires limited additional bond purchases to keep the targeted yield within the targeted range, and attenuates the impact of short-rate changes in the yield curve. In the absence of YCC, the effect of bond demand and supply on bond yields increases once again as the influence of the effective lower bound on nominal interest rates weakens.

JEL classification: E43, E52, E58, G12
Keywords: monetary policy, yield curve control, preferred habitat

* The authors are grateful to Kazuo Ueda and colleagues at the Bank of Japan for comments and discussions. Views expressed in the paper are those of the authors and do not necessarily reflect those of the Bank of Japan.
† Waseda University (email: jkoeda@waseda.jp)
‡ Monetary Affairs Department (currently Personnel and Corporate Affairs Department)

1. Introduction

Yield curve control (YCC), a policy that targets or caps one or more particular yields, has been implemented by several central banks.[1] However, there are few studies on YCC that clarify its mechanism. This paper attempts to analyze how yield curves are formulated under YCC using data from Japan, which has been actively implementing YCC since September 2016. Understanding this mechanism can help us examine the effectiveness of YCC and the impact on the yield curve of changes in the Bank of Japan's (BOJ) YCC.

One natural candidate to explain the YCC mechanism is a preferred habitat theory, which explicitly links bond demand and supply to interest rates at different maturity. More recently, Vayanos and Vila (2021, VV henceforth) explicitly incorporate the concept of preferred habitat into an asset pricing framework.[2] In this framework, if the central bank is treated as a price-elastic preferred habitat investor, the degree of price elasticity may be interpreted as the strictness of its YCC. Further, the degree of price elasticity may depend on the level of the targeted bond yield.

Our paper provides a preferred habitat view of YCC, extending VV's term structure model allowing the price elasticity of government bond demand by the central bank to depend on a targeted yield. The degree of price elasticity is allowed to increase substantially when the targeted bond yield approaches or exceeds the cap.[3] The resulting bond yields are no longer affine in yield-curve factors unlike VV in which bond yields are affine in these factors. The model parameters other than those that are directly related YCC are calibrated using various Japanese data mostly prior to the implementation of YCC in 2016. To analyze the effect of YCC on government bond yields, using these calibrated parameter values, we then simulate the model with different degrees of price elasticity.

Our model simulation sheds light on why yield targeting may require a small amount of bond purchases to achieve its targeted yield, as suggested by, for example, Bernanke (2016). We find that when the YCC is strictly implemented, supply factor risks are contained, and as a result, yield curves can flatten even with limited additional bond purchases. When YCC is absent, on the other hand, as the expected short-term interest rates increase, bond yields become more sensitive to the supply-factor, because the effect of an effective lower bound (ELB) on nominal interest rates weakens to some degree.

There have been developments in the literature whereby a preferred habitat framework is applied to the analysis of the effects of unconventional monetary policy.[4] VV examine the effects of

---

[1] Actual implementation of the control of government bond prices or yields varies across these central banks: the Federal Reserves during and after the WWII capped yields across the yield curve (Federal Reserve Board, 2020), the Reserve Bank of Australia (RBA) introduced a target for the yield on the 3-year Australian government bond from March 2020 to November 2021 (RBA, 2021), and the Bank of Japan has been controlling the long-term interest rate (ten-year government bond yield) as well as the shot-term interest rate since September 2016. In this paper, unless otherwise noted, the framework of the control of government bond prices or yields by central banks, regardless of its form, is referred to as YCC.

[2] After VV appeared as an NBER working paper in 2009 and became discussed in academic circles, it was finally published in one of the most influential economics journals, Econometica.

[3] In Japan, the current targeted maturity is 10 years, with the cap set at 25 basis points (BOJ, 2022).

[4] While Wallace's (1981) neutrality was an influential proposition for a long time in academic circles, the effect of government bond purchases by the central bank on bond yields has been analyzed assuming that bonds with different

assets purchases and forward guidance but does not analyze YCC. King (2019) introduces an ELB on nominal interest rates to the framework assuming a price-inelastic central bank, and analyzes the relationship between the effects of asset purchases and forward guidance and the ELB. Hamilton and Wu (2012) propose and estimate a discrete time version of VV assuming the preferred habitat investors' government bond demand is an affine function of the yield. The effects of the BOJ's bond purchases are quantified by Fukunaga et al. (2015), who also estimate a discrete time version of VV, and Sudo and Tanaka (2021), who analyze a dynamic stochastic general equilibrium model assuming imperfect substitutability between short- and long-term bonds. On the other hand, there are only a few studies on YCC, though Keynes (1936) refers to it as a possible monetary policy framework.[5] Recently, Lucca and Wright (2022) examine an Australian yield target and identify "narrow" liquidity channels with attention to high-frequency disconnections between the Australian government bond yield curve and the overnight indexed swap curve.[6] The YCC studies on Japan to date also focus on analyzing high-frequency market data and empirically confirm the existence of market segmentation consistent with a preferred habitat hypothesis.[7]

This paper proceeds as follows. Section 2 provides a brief history of YCC in Japan. Section 3 presents a simple model that highlights some key mechanisms of the preferred-habitat model of term structure of interest rates. Section 4 proposes a full-fledged model. Section 5 describes how model parameters are calibrated. Section 6 discusses the main results. Section 7 concludes.

2. YCC in Japan

In September 2016, the BOJ added YCC to the Quantitative and Qualitative Monetary Easing framework (QQE with YCC, hereafter), based on the Comprehensive Assessment (BOJ, 2016). Officially, the BOJ's QQE with YCC has the following three aims (BOJ, 2021): "The first, in order to achieve the price stability target of 2 percent, is to maintain the output gap in positive territory for as long as possible, given that the formation of inflation expectations in Japan is largely adaptive. The second is to introduce a framework in which the Bank controls interest rates to appropriate levels while taking into consideration both the positive and side effects of monetary easing, with the expectation that monetary easing will be prolonged. The third is to strengthen the forward-looking element of inflation expectations formation with the inflation-overshooting commitment."

maturities are imperfect substitutes (e.g., Tobin, 1969) and increasingly recognized among policy makers (e.g., D'Amico and King, 2013).

[5] As cited by Kuroda (2021b), Keynes (1936) refers to the possibility of yield curve control as a monetary policy framework as follows: "Perhaps a complex offer by the central bank to buy and sell at stated prices gilt-edged bonds of all maturities, in place of the single bank rate for short-term bills, is the most important practical improvement which can be made in the technique of monetary management."

[6] In addition to the "narrow" liquidity channels, Lucca and Wright (2022) also analyze "broad" transmission channels which capture duration and portfolio-balance effects. Following VV, we focus on the "broad" transmission channels assuming that the non-pecuniary marginal costs for government bonds which generate the "narrow" liquidity channels in Lucca and Wright (2022) are small in general.

[7] Using high-frequency data, Hattori and Yoshida (2021) and Ito (2019) examine the time-series properties of JGB yield and interest-rate swap rates under the BOJ's YCC.

Under QQE with YCC, the BOJ sets the levels of short- and long-term interest rates as the operating targets in the guideline for market operations, instead of the amount of increase in the monetary base and the amount of JGB purchases, as used in previous frameworks. The BOJ facilitates the formation of a yield curve that is considered most appropriate for maintaining the momentum toward achieving the price stability target of 2 percent, taking account of developments in economic activity and prices as well as financial conditions (Kuroda, 2017). Specifically, the BOJ has maintained the short-term policy interest rate at minus 0.1 percent and the target level of the 10-year JGB yields at around 0 percent since the introduction of QQE with YCC.

BOJ (2021) points out that the QQE with YCC has had positive effects on financial markets and the macro economy. At the same time, it also notes that the functioning of the JGB market has decreased since the introduction of YCC with the range of fluctuations in interest rates having narrowed. In July 2018, in order to enhance the sustainability of QQE with YCC, the BOJ made the conduct of JGB purchases more flexible, making clear that 10-year JGB yields might move upward and downward to some extent, mainly depending on developments in economic activity and prices. Specifically, regarding the range of fluctuations in 10-year JGB yields, the BOJ announced that it would allow 10-year JGB yields to move upward and downward over about double the previous range of between around plus and minus 0.1 percent. In March 2021, given that the range of actual fluctuations in interest rates had frequently narrowed, the BOJ made clear that the range of 10-year JGB yield fluctuations would be between around plus and minus 0.25 percent to strike an appropriate balance between maintaining market functioning and controlling interest rates (Kuroda, 2021a).

Since the introduction of YCC, the BOJ has added a number of novel operations. In September 2016, to stop a significant rise in interest rates, it introduced the fixed-rate purchase operations, through which it purchases an unlimited amount of JGBs with certain maturities at fixed rates. In March 2021, with a view to further strengthening the fixed-rate purchase operations, the BOJ introduced "fixed-rate purchase operations for consecutive days," through which it conducts the fixed-rate purchase operations consecutively for a certain period of time. More recently, in April 2022, to clarify how the BOJ conducts fixed-rate purchase operations for consecutive days, the BOJ announced that it would offer to purchase 10-year JGBs at 0.25 percent every business day through fixed-rate purchase operations, unless it was highly likely that no bids would be submitted.

There are several views about the Japanese YCC in central banking circles. Just after the BOJ announced the introduction of YCC, former Fed chairman Ben Bernanke expressed his view that the BOJ would be able to meet its yield target by purchasing considerably less than 80 trillion yen of JGBs a year, the target quantity for JGB purchases at that time (Bernanke, 2016). He pointed out the "credibility" of YCC as the reason for a small amount of JGB purchases. If YCC were not credible, that is, if market participants had expected "the pegging on the long-term yield" to be abandoned in the near term, bondholders would have a strong incentive to sell as quickly as possible, and the BOJ could find itself owning most or all of the eligible securities. However, Bernanke argued that the risk of losing the credibility was manageable in Japan. Similar to Bernanke's view, the minutes of the

Federal Open Market Committee (Federal Reserve Board, 2020) mention that credible yield curve cap or target policies "can control government bond yields, pass through to private rates, and, in the absence of exit considerations, may not require large central bank purchases of government debt." In a similar vein, Higgins and Klitgaard (2020) cite the Japanese experience of YCC as an illustration that a central bank can exert fairly close control over the term structure of interest rates without large-scale interventions in the government bond market. The reason given in that paper is that market participants accept that the bank will buy whatever quantity of government bonds necessary to keep yields from rising above the target. Carlson et al. (2020) also point out that soft ceilings on yields, as opposed to firm or strict ceilings, might not necessarily result in a smaller overall balance sheet. In their view, softer ceilings cannot stop yields rising above the ceilings, which trigger purchases of securities with maturities covered by the ceilings at a particular pace until yields move below the ceiling.

In this paper, we modify and calibrate a canonical preferred-habitat model of term structure of interest rates to fit the model to the Japanese experience and examine the mechanism of YCC focusing on the credibility or strictness of YCC, which is viewed in these existing studies as its most important feature.

3. Simple example

In this section, we use a simple three-period model (t = 0, 1, 2) to illustrate how the degree of price elasticity of preferred habitat's government bond demand affects the long-term rate in an almost static setting. Although the model is simplified, it has the basic features of the VV model.

Agents are of two types: arbitrageurs and preferred-habitat investors. Arbitrageurs can invest both in short-term (one-period) and long-term (two-period) bonds in period 0, they can only invest in the short-term bond in period 1, and they cannon make any investments in period 2. The prices of short-term (one-period) and long-term (two-period) bonds in period t are denoted as $P_t(1)$ and $P_t(2)$ respectively.

Arbitrageurs maximize their one-period gross mean-variance return where W_t is their wealth in period t and W_{t+1}/W_t is their gross return. Their initial period wealth W_0 is normalized at 1. Their maximization problem (eq. (1)) is to choose their holdings of short- and long-term bonds in period 0, denoted as $X_0(1)$ and $X_0(2)$ respectively. $X_0(1)$ and $X_0(2)$ add up to 1 as they are expressed in the shares of W_0,

$$\max_{X_0(1),X_0(2)} E_0[R_1] - \frac{a}{2} Var_0[R_1], \text{ s.t. } R_1 \equiv \frac{W_1}{W_0} = \frac{1}{P_0(1)} X_0(1) + \frac{P_1(1)}{P_0(2)} X_0(2), \; X_0(1) + X_0(2) = 1. \tag{1}$$

The above maximization problem can be rewritten as

$$\max_{X_0(2)} e^{r_0}(1 - X_0(2)) + E_0\left[\frac{P_1(1)}{P_0(2)} X_0(2)\right] - \frac{a}{2} Var_0\left[\frac{P_1(1)}{P_0(2)} X_0(2)\right] \tag{2}$$

where $P_0(1) \equiv \exp(-\max\{r_0, b\})$, $P_1(1) \equiv \exp(-\max\{r_1, b\})$ with $r_1 \sim N(\mu_r, \sigma_r^2)$, and the short rate r_t is assumed to be controlled by the central bank. The first-order condition is given by

$$X_0(2) = \frac{E_0\left[\frac{P_1(1)}{P_0(2)}\right] - e^{r_0}}{aVar_0\left[\frac{P_1(1)}{P_0(2)}\right]} = \frac{-e^{r_0}P_0(2)^2 + E_0[e^{-r_1}]P_0(2)}{aVar_0[e^{-r_1}]}.$$

The preferred-habitat investors consist of the central bank and other preferred habitat investors whose long-term bond demand is given by

$$\tilde{Z}_0(2) = -\alpha \log P_0(2) - \tilde{\beta}, \tag{3}$$

where α is the price semi-elasticity of their bond demand and $\tilde{\beta}$ is the demand intercept. Regarding bond supply, the government exogenously supplies both long- and short-term bonds in period 0, denoted as $S_0(2)$ and $S_0(1)$ respectively, and the short-term bond in period 1. $S_0(2)$, $S_0(1)$, and $\tilde{Z}_0(2)$ are expressed in the shares of W_0.

Imposing the market clearing condition, i.e., $S_0(2) = \tilde{Z}_0(2) + X_0(2)$, and combining the first-order condition and the demand equation (eq. (3)), the following equation of long-term rate, $Y_0(2)$, can be derived

$$Y_0(2) \approx \frac{r_0 + E_0[r_1]}{2(1 + a\alpha Var_0[r_1])} + \frac{aVar_0[r_1]}{2(1 + a\alpha Var_0[r_1])}\left(S_0(2) + \tilde{\beta}\right) \tag{4}$$

Eq. (4) holds approximately as we impose the approximation of $e^x \approx 1 + x$. It highlights the key intuitions of the VV model as illustrated in Figures 1a-d which plot the long-term bond supply curve ($S_0(2)$, the dotted black lines) and the demand curve ($\tilde{Z}_0(2)$+$X_0(2)$, the sloping blue lines and red dashed lines). The supply curve is vertical as the government bond issuance is exogenous. The demand curve is upward sloping with the long-term interest rate ($Y_0(2)$) plotted on the y-axis. Figure 1a illustrates that an increase in the long-term bond supply ($S_0(2)$), which shifts the supply curve to the right, increases the long-term interest rate ($Y_0(2)$). Figure 1b shows that a decline in the short rate (r_0), which shifts the demand curve down to the right and lowers the long-term rate. Figure 1c shows the effect of the ELB on nominal interest rates, which reduces short-rate volatility ($Var_0[r_1]$). Without the ELB, the demand curve steepens, compared with when the ELB is present, and as a result, the supply effect on the long-term rate increases. Figure 1d illustrates that the higher the price semi-elasticity of their bond demand, the flatter the demand curve, and as a result, the lower the supply effect on the long-term rate becomes. In other words, the supply effect on the long-term rate becomes weaker under the stricter YCC (the strictness increases with α), even when α does not depend on the level of bond yields,.

Our three-period model, however, does not address the dynamic effects of yield-curve factors on bond yields. Thus, to quantify the YCC effect on bond yield, we propose the full-fledged term-structure model set forth in the next section.

Figure 1: Supply and demand curves in the simple three-period model

a) An increase in long-term bond supply

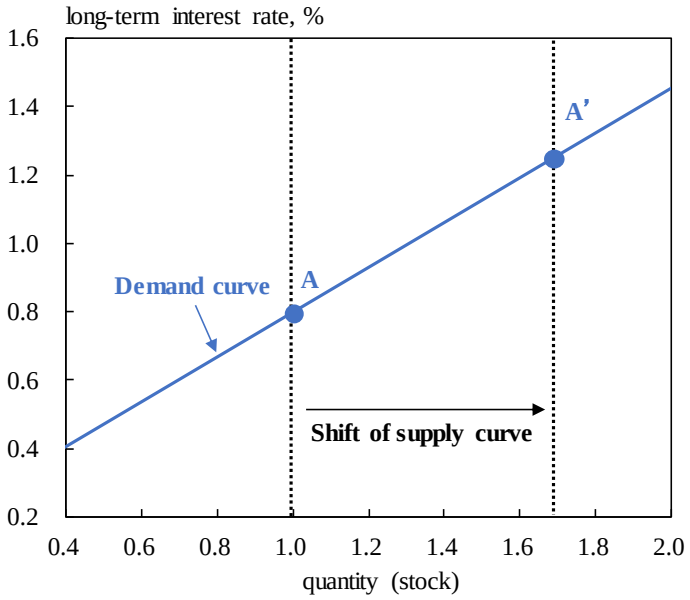

b) A decline in the short rate

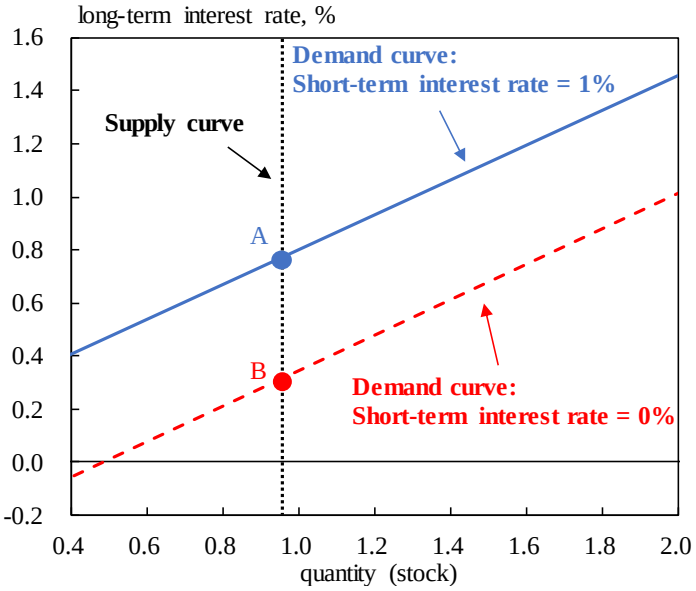

c) Effect of ELB on nominal interest rates

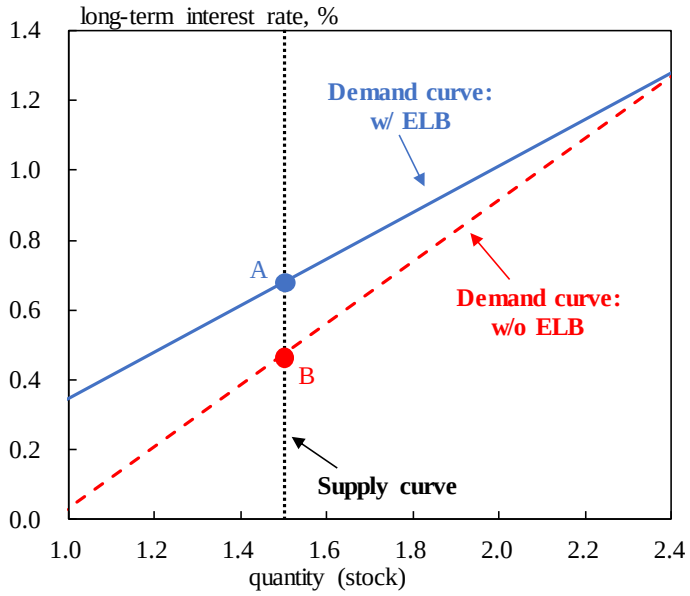

d) An increase in YCC strictness

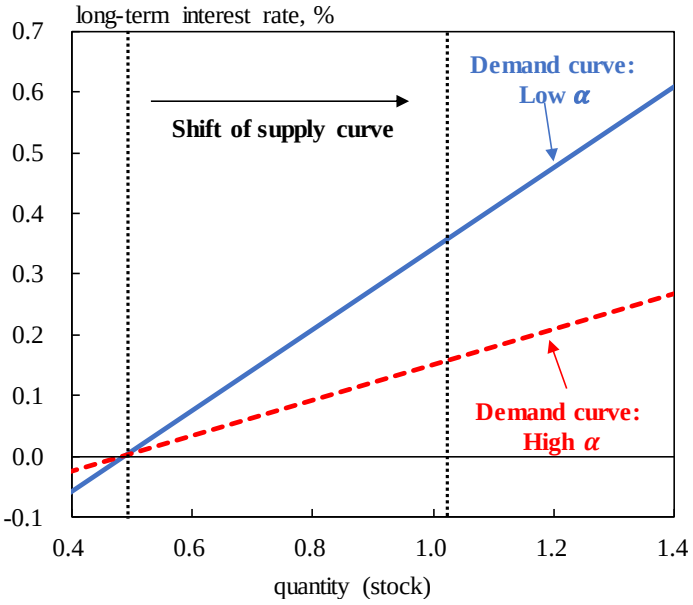

Note: Figures 1a-d depict the supply and demand curves implied in the simple three period model. For illustration, we set $r_0 = 0.01, \alpha = 4, \beta = -2, a = 50, \mu_r = \sigma_r = 0.02$ with ELB on nominal interet rates ($b = 0$), depicted by the solid blue lines in Figures 1a-c. Only r_0 is changed to 0 for the red dashed line in Figure 1b. Only r_0 and b are changed to 0 and $-\infty$ respectively for the red dashed line in Figure 1c. We also set $r_0 = 0$, $\beta = -2$, $a = 50$, $\mu_r = \sigma_r = 0.02$ with $b = 0$ in Figure 1d with different values of α (specifically, α equals 4 and 100). An increase in the price elasticity of preferred habitat (Figure 1d) is assumed to increase the degree of YCC strictness.

4. The Model

The benchmark model is the same as the VV model, except that it extends it by (i) allowing α to

depend on bond maturity and yield to explicitly model YCC, (ii) including an ELB on nominal interest rates, and (iii) correlating the two factor shocks to capture the empirical properties of the Japanese data. Since (i) and (ii) are highly nonlinear in nature, we consider them separately. We denote the model that incorporates (i) and (iii) as VV-Alpha, and the model that incorporates (ii) and (iii) as VV-ELB. VV-ELB is the same as the model presented by King (2019) except that we allow for (iii).

Let $P_t(\tau)$ denote the time-*t* price of a government bond with remaining maturity τ and $\mathrm{y_t}(\tau)$ denote the corresponding time-*t* bond yield which is related to the price by $\mathrm{y_t}(\tau) = -\log P_t(\tau)/\tau$. As in the previous section, there are two types of agents: arbitrageurs and preferred habitat investors.

Arbitrageurs can invest in the bonds and in the short rate. Their time-t wealth (W_t) evolves according to

$$dW_t = \int_0^\infty x_t(\tau)\frac{dP_t(\tau)}{P_t(\tau)}d\tau + \left(W_t - \int_0^\infty x_t(\tau)d\tau\right)r_t dt, \tag{5}$$

where $x_t(\tau)$ is the market-value quantity of the bond at maturity τ that they choose to hold, and r_t is the short rate. Arbitrageurs have mean-variance preferences and solve the following optimization problem,

$$\max_{x_t(\tau)\forall\tau} E_t^{\mathcal{P}}[dW_t] - \frac{a}{2}Var_t^{\mathcal{P}}[dW_t], \qquad a \geq 0, \tag{6}$$

subject to eq. (5), where a is absolute risk aversion that characterizes the trade-off between mean and variance. $E_t^{\mathcal{P}}$ and $Var_t^{\mathcal{P}}$ represent expectation and variance conditional on the time-*t* state. The superscript $\mathcal{P}$ indicates the physical probability measure. The first-order conditions for this problem can be written as follows.

$$E_t^{\mathcal{P}}\left[\frac{dP_t(\tau)}{P_t(\tau)}\right] = r_t dt + a\ Cov_t^{\mathcal{P}}\left[\frac{dP_t(\tau)}{P_t(\tau)}, \int_0^{T^*} x_t(s)\frac{dP_t(s)}{P_t(s)}ds\right], \tag{7}$$

where $Cov_t^{\mathcal{P}}$ represents covariance conditional on the time-*t* state.

The preferred-habitat investors demand a time-varying quantity of government bonds $\tilde{z}_t(\tau)$ at each maturity,

$$\tilde{z}_t(\tau) = -\alpha\big(\tau, P_t(\tau)\big)\log P_t(\tau) - \tilde{\beta}_t(\tau), \tag{8}$$

where the slope coefficient α can depend on maturity τ as well as government bond price or yield. Following VV, we assume that government bonds are in zero supply. This is without loss of generality since we can define the function of the net supply $z_t(\tau)$ as the supply by the government for the bond maturity τ net of the preferred habitat demand. Eq. (8) can be rewritten as follows.

$$z_t(\tau) = \alpha\big(\tau, P_t(\tau)\big)\log P_t(\tau) + \beta_t(\tau),$$

where the net supply intercept $\beta_t(\tau)$ depends on both *t* and τ and takes the following form

$$\beta_t(\tau) = \theta_0(\tau) + \theta(\tau)\beta_t. \tag{9}$$

We define β_t as the net supply-risk factor which does not depend on maturity. The value of α represents the price semi-elasticity of bond net supply. When the τ period bond price decreases by

one percent, $z_t(\tau)$ drops by α, other things being equal. In the context of YCC, we interpret the value of α as the strictness of YCC, assuming that the central bank is the dominant preferred habitat investor. Specifically, we represent the α-function under YCC as follows.

$$\alpha\big(\tau, P_t(\tau)\big) = \begin{cases} \alpha & \text{if } \tau = \tau^* \text{ and } y_t(\tau) \geq y^* \\ 0 & \text{otherwise} \end{cases}, \tag{10}$$

where τ^* is the targeted maturity and y^* is the cap on the targeted-maturity yield.

There are two yield-curve factors, the short rate and the net supply-risk factor. When the economy faces an ELB constraint or when b is sufficiently low, the short rate is the maximum of the shadow rate ($\hat{r}_t$) and a lower bound b (i.e., $r_t = \max(\hat{r}_t, b)$). Otherwise, in the absence of the ELB constraint, the short rate and the shadow rate are equal (i.e., $r_t = \hat{r}_t$).

The factor dynamics of the shadow rate and the net supply-risk factor (β_t) are assumed to follow the Ornstein-Uhlenbeck process under the $\mathcal{P}$-measure,

$$d\hat{r}_t = \kappa_r(\mu - \hat{r}_t)dt + \sigma_r dB_{r,t} \text{ and } d\beta_t = -\kappa_\beta \beta_t dt + \sigma_\beta dB_{\beta,t}. \tag{11}$$

The factor dynamics under the $\mathcal{Q}$ (risk neutral)-measure are assumed to be,

$$d\hat{r}_t = \mu_r^{\mathcal{Q}}(\hat{r}_t, \beta_t)dt + \sigma_r dB_{r,t} \text{ and } d\beta_t = \mu_\beta^{\mathcal{Q}}(\hat{r}_t, \beta_t)dt + \sigma_\beta dB_{\beta,t}. \tag{12}$$

We solve for government bond prices under the $\mathcal{Q}$-measure. The government bond pricing function can be generally expressed as follows

$$P_t(\tau) \equiv f(\tau, \hat{r}_t, \beta_t) = f(T - t, \hat{r}_t, \beta_t) = E_t^{\mathcal{Q}}\left[e^{-\int_t^T r_u du}\right], \tag{13}$$

where T indicates the period that τ period bond matures.

As derived in Appendix A, applying Ito's lemma and combining no-arbitrage and first-order conditions, and the net supply function, the following expression for the drift terms is derived:

$$\begin{bmatrix} \mu_r^{\mathcal{Q}}(\hat{r}_t, \beta_t) \\ \mu_\beta^{\mathcal{Q}}(\hat{r}_t, \beta_t) \end{bmatrix} \begin{bmatrix} \kappa_r(\mu - \hat{r}_t) \\ -\kappa_\beta \beta_t \end{bmatrix} \tag{*}$$

$$= -a \begin{bmatrix} \sigma_r^2 & \rho\sigma_r\sigma_\beta \\ \rho\sigma_r\sigma_\beta & \sigma_\beta^2 \end{bmatrix} \begin{bmatrix} \int_0^\infty \frac{\big(\theta_0(s) + \alpha\big(s, f(s, \hat{r}_t, \beta_t)\big)\log f(s, \hat{r}_t, \beta_t) + \theta(s)\beta_t\big)}{f(s, \hat{r}_t, \beta_t)} f_r(s, \hat{r}_t, \beta_t)ds \\ \int_0^\infty \frac{\big(\theta_0(s) + \alpha\big(s, f(s, \hat{r}_t, \beta_t)\big)\log f(s, \hat{r}_t, \beta_t) + \theta(s)\beta_t\big)}{f(s, \hat{r}_t, \beta_t)} f_\beta(s, \hat{r}_t, \beta_t)ds \end{bmatrix},$$

where ρ is the correlation between the factor shocks. Eq. (*) plays a crucial role in solving the model under the $\mathcal{Q}$-measure. Eq. (*) also implies that the value of α affects the bond yield by changing the risk premia, because α shows up only in the second term on the right-hand side equation and disappears when risk-neutrality (a=0) is assumed. The model reduces to VV when $\alpha\big(\tau, P_t(\tau)\big)$ is constant in the absence of ELB on nominal interest rates. The bond yields in VV-Alpha or VV-ELB are no longer affine and they are solved using the numerical algorithm explained in Appendix B.

5. Calibration

To obtain parameter values that fit the Japanese case, we calibrate model parameters using the maturity structure data of Japanese government bonds, zero coupon bond yields, and survey data on the 3-month Tokyo Interbank Offered Rate (TIBOR).[8] The data sample covers a period prior to the introduction of YCC and the negative interest rate policy (NIRP), with the exception of the survey data, which are available only from January 2017, and is used to calibrate the shadow rate dynamics. A description of the data is provided in Appendix C.

We calibrate VV-ELB given that the sample period covers a period during which an ELB constraint appears to be present. BOJ (2016) points out that the interest rate of excess reserves worked as a floor (ELB) from 2014, prior to the implementation of NIRP in early 2016. The VV-ELB model parameters consist of the coefficients in the maturity structure equation (θ_0, θ), the coefficients in the factor dynamics $(\mu, \kappa_r, \sigma_r, \kappa_\beta, \sigma_\beta)$, and the remaining parameters (b, ρ, a, α). We normalize the value of σ_β by setting it equal to 0.01. We set $\alpha = 0$ due to the lack of empirical evidence indicating that it is statistically different from zero prior to the YCC implementation in September 2016.[9] We also set b equal to 0 in the benchmark calibration.

To estimate the maturity-structure coefficients, we proxy β by the first PCA component on the maturity-structure variables (i.e., the bonds outstanding by remaining maturity years as a ratio of GDP). We denote this PCA component as $\hat{\beta}$, which explains 91% of the variations in the maturity-structure variables. As depicted in Figure 2, during the financial crisis in the late 1990s, $\hat{\beta}$ jumped, and it then continued to increase in the 2000s. After the global financial crisis, however, it started to decline following large BOJ's asset purchases under the QQE. During FY2020 (April 2020-March 2021) amid the COVID-19 pandemic, it started to increase again. We calibrate θ by the factor loadings of $\hat{\beta}$ as shown in Figure 3, and θ_0 by the sample averages of the maturity structure variables as shown in Figure 4, since the mean of β is normalized to be zero in the model. The coefficient regarding the β-dynamics (κ_β) is calibrated by regressing $\hat{\beta}$ on its lag.

[8] The survey data on the 3-month Tokyo Interbank Offered Rate are taken from Consensus Economics Inc., "Consensus Forecast."

[9] Despite the continued decline in the long-term rates, as discussed, for example, by Fukunaga et al. (2015), Japanese private preferred habitat investors, especially life insurance companies, steadily increased their holdings of JGBs with maturities over 10 years during the 2000s, in order to match the duration of their assets and liabilities under the regulations and accounting standards that forced them to reduce their holdings of risky assets. Further, Koeda and Kimura (2022) do not find empirical evidence that supports a positive value of α.

Figure 2: The first PCA component on the maturity-structure variables ($\hat{\beta}$)

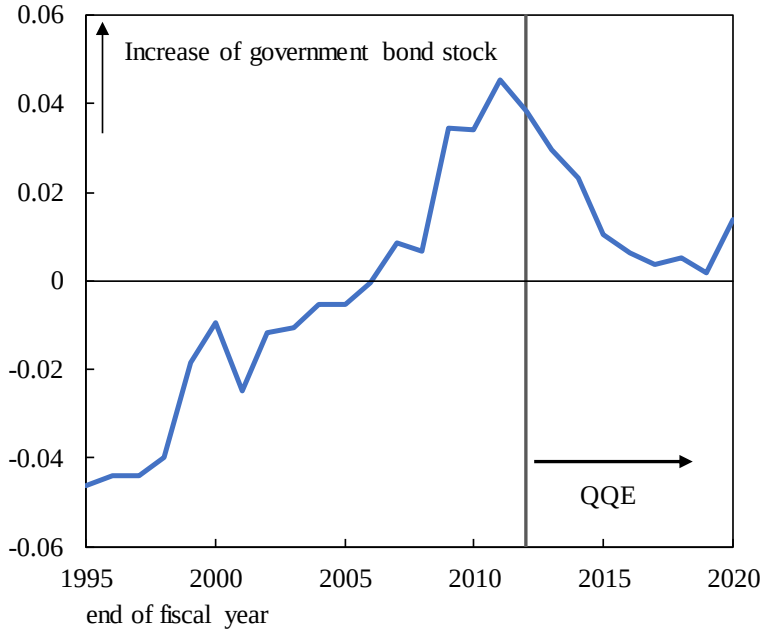

Note: This figure plots the first PCA component extracted from the maturity structure variables (i.e., the bonds outstanding by remaining maturity years as a ratio of GDP).

Figure 3: The loadings of $\hat{\beta}$ (calibrated θ)

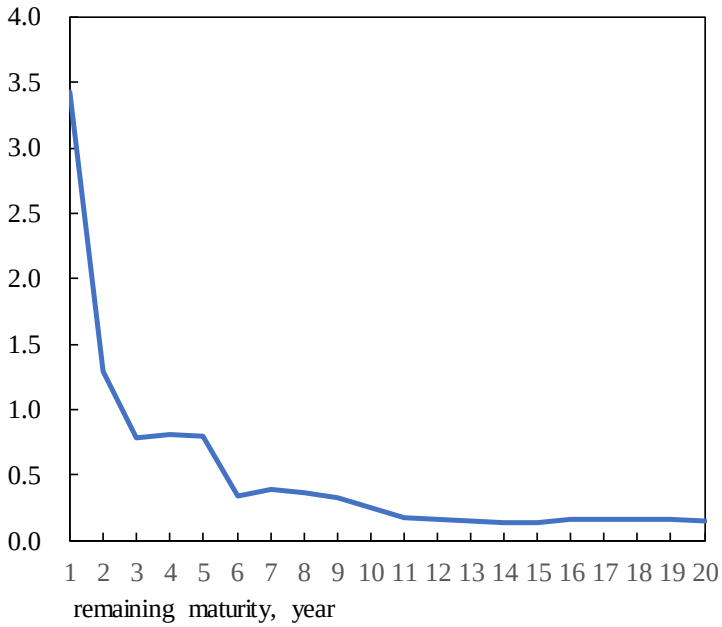

Note: This figure plots the loading of the first PCA compoment extracted from the maturity structure variables.

Figure 4: Calibrated θ_0

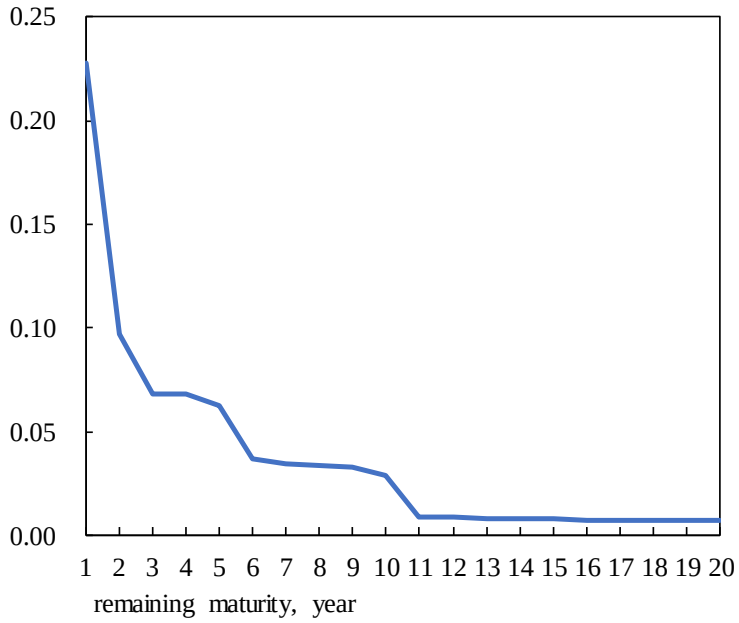

Note: This figure plots the sample averages of the maturity structure variables for each remaining year of maturity.

The coefficients regarding the short rate dynamics $(\mu, \kappa_r, \sigma_r)$ are estimated using the survey data on 3-month TIBOR. We iterate forward the short-rate equation under the $\mathcal{P}$ measure (eq. (12)). We then analytically derive the conditional expectations and variances of short rates, which are used to estimate μ, κ_r and σ_r. We assume that the ELB constraint is not perceived by the market participants sufficiently far ahead in the future, specifically over 4 years. The level difference between TIBOR rates and government bond yields of comparable maturity is also adjusted based on the historical averages of the level differences.

The remaining parameters (ρ and α) are estimated via an extended Kalman filter with the observation equation approximated by

$$\boldsymbol{y}_t = \boldsymbol{f}(\hat{r}_t, \beta_t) + \boldsymbol{w}_t,$$

where

$$\boldsymbol{f}(\hat{r}_t, \beta_t) \approx \boldsymbol{f}\big(\hat{E}[\hat{r}_t|\beta_t, \mathcal{F}_{t-1}], \beta_t\big) + \frac{\partial \boldsymbol{f}}{\partial r}\big(\hat{E}[\hat{r}_t|\beta_t, \mathcal{F}_{t-1}], \beta_t\big)\big(\hat{r}_t - \hat{E}[\hat{r}_t|\beta_t, \mathcal{F}_{t-1}]\big),$$

and the state equations given by eq. (12). We treat $\hat{r}_t$ as a latent variable and β_t as an observed variable. $\hat{E}[\hat{r}_t|\beta_t, \mathcal{F}_{t-1}]$ is a linear projection of $\hat{r}_t$ on β_t and information set in period t-1 ($\mathcal{F}_{t-1}$). Appendix D provides details of our extended Kalman filtering method following Harvey (1989).

Table 1 reports the calibrated parameter values. The negative value of ρ (-0.29) indicates that the net supply shocks are negatively correlated with the short-rate shocks in Japan. This negative correlation is crucial to explain the continued government debt expansion in light of the low interest rate environment in Japan. The value of α (15.1) is higher than the one calibrated for the US by VV, but it is comparable to the value estimated for Japan by Koeda and Kimura (2022), suggesting that the

arbitrageurs in Japan are more risk averse than those in the US.

Table 1: Calibrated parameters

μ	0.0065
κ_r	0.2256
σ_r	0.0136
a	15.0675
ρ	-0.2852
κ_β	0.1453

Note: This table reports calibrated parameter values for VV-ELB. The ELB (b) and α are set at 0. σ_β is normalized at 0.01. The calibrated values for θ and θ_0 are reported in Figures 3-4.

6. The Main Results

To investigate the effect of YCC on bond yields, we numerically solve VV-Alpha for different values of α setting the targeted maturity (τ^*) at 10 years and the cap on the targeted maturity yield (y^*) at 0.25 percent to be consistent with the recent Japanese YCC experience discussed in Section 2. We keep the same calibrated structural parameters in the factor dynamics and maturity structure equations as those calibrated for VV-ELB in the previous section.

Figure 5 shows the model simulation results with different values of α. The values of the two factors ($\hat{r}$ and β) are set at -0.1% and the end-March 2021 estimate, respectively. According to the results, when the YCC is very strict, say $\alpha = 20$, the yield curve flattens allowing the targeted yield to be within the targeted range (red dashed line). Contrary to the result from the simple example in Section 3, this flattening can occur without additional BOJ bond purchases as long as the market participants believe in sufficiently strict YCC, i.e., BOJ's bond purchase commitment to keep the targeted rate below the cap is sufficient. On the other hand, when the YCC is soft, say $\alpha = 1$, the yield curve steepens and the targeted bond yield exceeds the cap even when additional BOJ bond purchases are made (solid blue line in Figure 5).

Figures 6 and 7 plot factor loadings for government bond yields against maturity with respect to the net supply factor β_t, and the shadow rate $\hat{r}_t$. Specifically, as in King (2019), the partial derivatives of each bond yield with respect to factors are presented. The values of the two factors ($\hat{r}$ and β) are the same as those in Figure 5. The figures show that bond yields become less responsive to factor changes with a higher value of α, particularly in response to changes in the net supply-risk factor.

Figure 5: Model-simulated yield curves with different α

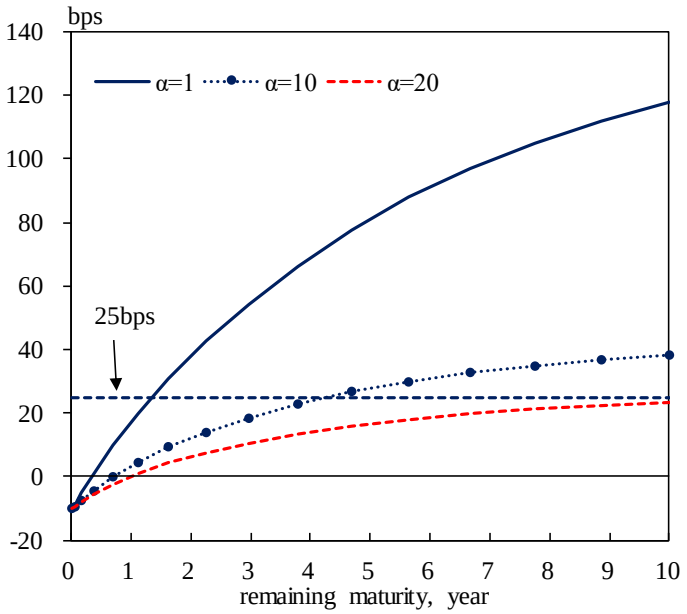

Note: This figure plots the model-simulated yields in VV-Alpha with different values of α in basis points. The horizontal axis is the remaining maturity in years. The values of the two factors ($\hat{r}$ and β) are set at -0.1% and the end-March 2021 estimate, respectively.

Figure 6: Factor loadings of net supply factor with different α

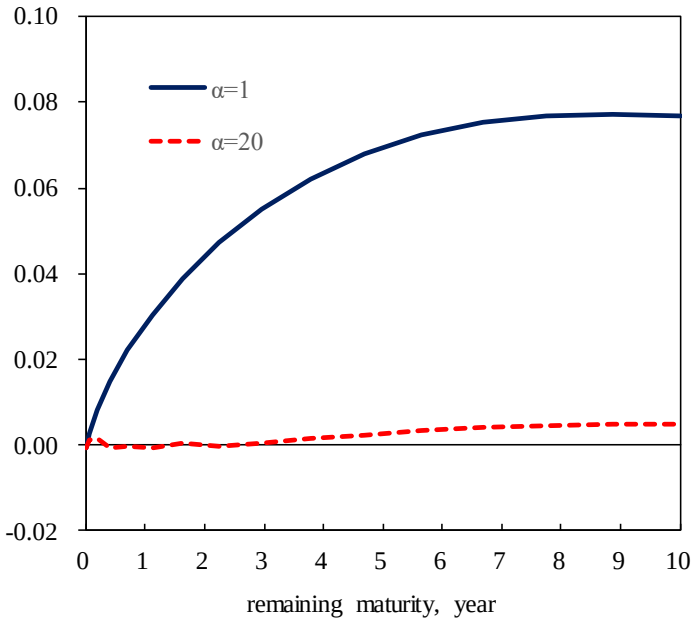

Note: This figure plots the partial derivatives of bond yields with respect to the net supply-risk factor. The factor values are the same as in Figure 5.

Figure 7: Factor loadings of shadow rate with different α

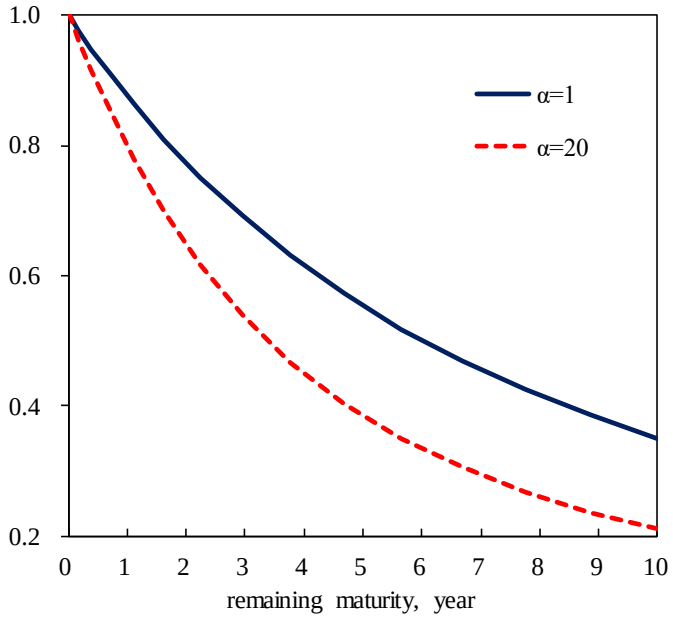

Note: This figure plots the partial derivatives of bond yields with respect to the short rate. The factor values are the same as in Figure 5.

Figure 8 shows the effect of additional bond supply on bond yield. The size of supply is set equal to 10% of GDP assuming the observed maturity-structure. Specifically, empirical correlation between $\hat{\beta}$ and the total net bond supply as a percentage of GDP ($\sum_{\tau=1}^{\tau=20} z_t(\tau)$) is employed. The solid blue line shows the difference in yield changes under strict YCC (α =20) and those under soft YCC (α =1). Negative values imply that yield changes under the soft YCC are larger than those under the strict YCC. The difference is mostly explained by the yield increase under the soft YCC because there is little change on the yield curve under the strict YCC as net supply factor risks are contained.

Figure 9 shows the effect of a 1-percent short-rate increase on bond yield. Specifically, it reports the difference in yield changes under strict and soft YCC. The difference implies that the yield increases due to the increase in the short-rate under the soft YCC are larger than those under the strict YCC. In other words, as long as sufficiently strict YCC is implemented, there is limited impact on the yield curve even when the short rate increases. The difference in yield changes becomes largest at the middle of the yield curve. At the long-end as well as the short-end of the yield curve, the strictness of YCC has less impact on the size of the effect of a short-rate increase. This is because when the short rate increases temporarily, given that it converges to its long-run value eventually, the degree of YCC strictness has little impact on bond yields at sufficiently long maturities.

Our simulation results based on Japanese data are consistent with Chaurushiya and Kuttner's (2003) findings about the Federal Reserve's targeting the yield curve between 1942 and 1951. They argue that even when the yield caps were not binding, the Fed's commitment to the caps limited bonds' downside price risk, helping to keep long-term yields low. They also emphasize that even after the short rate increased, the Fed's defense was successful under its credible commitment to the long-term

yield cap, despite its relatively small share in the overall long-term bond market.

Figure 8: The difference in the effect of BOJ bond purchases: strict vs. soft YCC

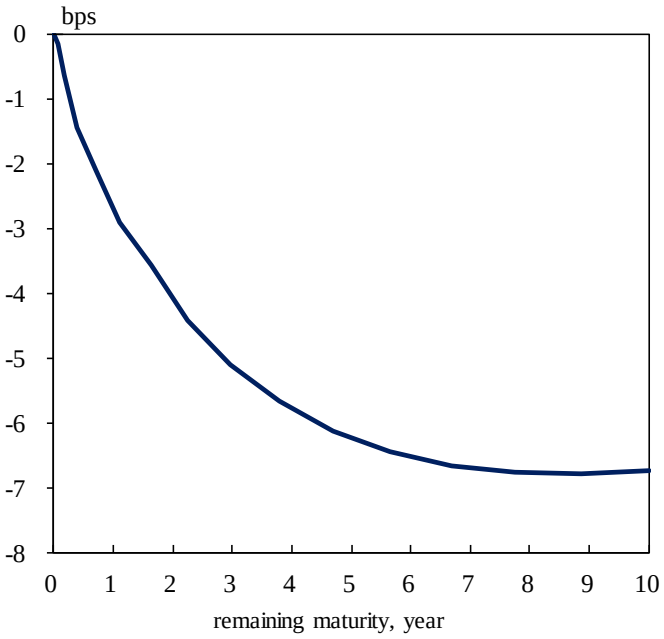

Note: This figure plots the difference between the model-simulated yield changes under strict YCC ($\alpha = 20$) and those with soft YCC ($\alpha = 1$) in response to a 10 percent increase in bond supply as a percentage of GDP. The factor values are the same as in Figure 5. The vertical axis is in basis points. The horizontal axis is remaining maturity in years.

Figure 9: The difference in the effect of short rate increases: strict vs. soft YCC

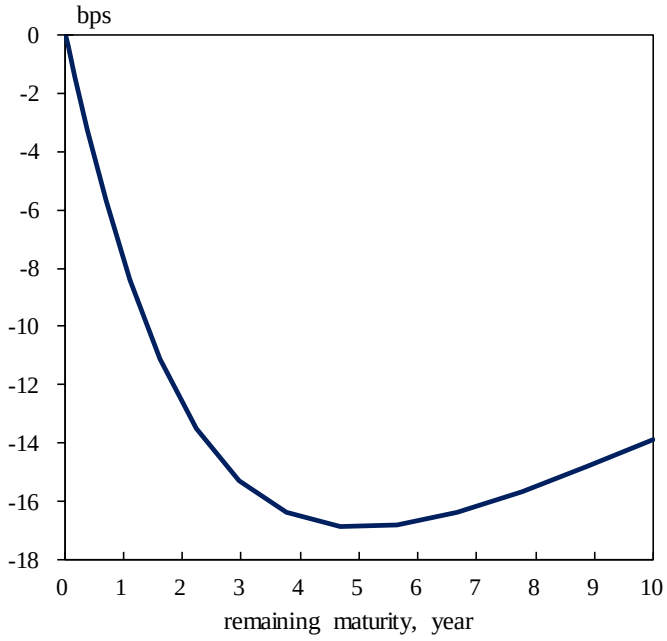

Note: This figure plots the difference between the model-simulated yield changes under strict YCC ($\alpha = 20$) and those with soft YCC ($\alpha = 1$) in response to a one percent increase in the short-rate. The factor values are the same as in Figure 8. The vertical axis is in basis points. The horizontal axis is remaining maturity in years.

It should be noted that VV-Alpha does not incorporate an ELB on nominal interest rates because it intends to analyze the YCC period during which the short rate is allowed to take negative values during the BOJ's NIRP period. Further, in March 2021, the BOJ established the Interest Scheme to Promote Lending framework which was intended to allow the nimbleness of the short-term policy rate to take more negative values (BOJ, 2021). On the other hand, the ELB constraint appears to be stronger prior to the introduction of NIRP in early 2016. The BOJ's Comprehensive Assessment (2016) states "the impact of a given increase in the Bank's JGB holdings on long-term JGB yields diminished between the start of 2014 and the introduction of the negative interest rate." It then points out the possibility that an ELB attenuates the impact of the additional bond purchases.

Existing studies support this attenuating effect. For example, King (2019) studies the case for the US and shows that a decline in the net supply factor proxy, measured by the maturity weighted debt to GDP, significantly lowered the 10-year zero coupon bond yield prior to December 2008, whereas no statistically significant effect is found since then. Grande, Grasso, and Zinna (2019) study the case for the euro area and show that increase in the share of government bond holdings by the central banks and other preferred-habitat investors lowered the 10-year euro-area OIS rate to a lesser degree during the ELB period which began in August 2012.

We have also confirmed this attenuating effect in our calibrated VV-ELB for Japan. Figure 10 plots the effect of additional BOJ bond purchases on bond yield when setting ELB at 0 percent. The size of purchases is set equal to 10% of GDP as in Figure 8. The longer the time before normalization (i.e., when the shadow rate is much lower relative to the ELB), the stronger the ELB attenuating effect, thus the weaker the bond yield responses to bond demand and supply changes. The magnitude of the BOJ bond purchase effect is broadly consistent with that quantified by Fukunaga et. al (2015) and Sudo and Tanaka (2021). The latter authors also find that the stock effects (the total amount of bonds taken away from the private sector) dominate the flow effects (the size of the bond purchases in each period).

Figure 10: The attenuating effect of ELB on the impact of additional BOJ bond purchases

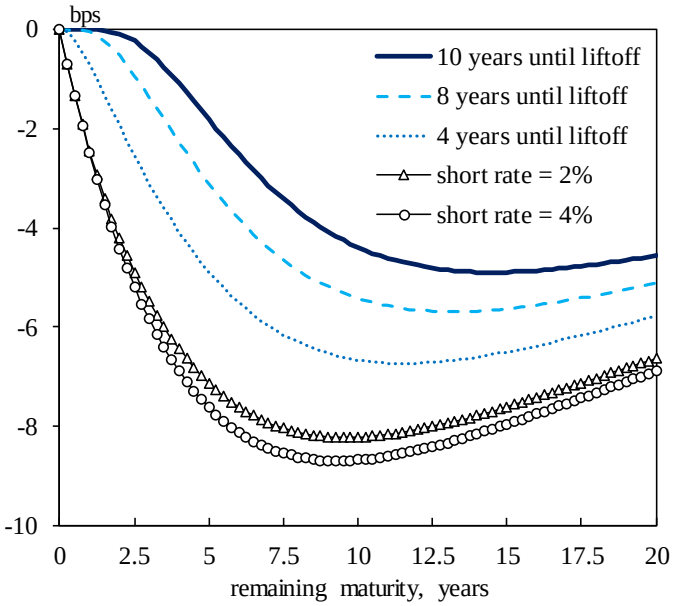

Note: This figure plots the effect of additional BOJ bond purchases on bond yield when setting ELB on nominal interest rates at 0 percent and $\beta = 0$. The size of purchases is set equal to 10% of GDP as in Figure 8. The larger the gap between the ELB and the shadow rate, the longer the timing for normalization. The vertical axis is in basis points. The horizontal axis is the remaning maturity in years.

7. Conclusion

We study how YCC works both theoretically and quantitatively using a preferred habitat term structure model. We construct a term structure model explicitly incorporating YCC and propose the numerical algorithm of the computation of bond prices in the model. To fit the model to the Japanese experience, we have calibrated the model parameters, exploiting various Japanese data including the maturity structure information of Japanese government bond markets and the survey data on interbank rates. The model simulations demonstrate that YCC can dampen the effect of net supply shocks on bond yield.

There are some tasks for future research and points to be noted. First, we have assumed that arbitrageurs and preferred-habitat investors are present over the same maturity range. However, if the arbitrageurs are at work on a narrower maturity range, then the bond markets that are outside of the range become fully segmented. Relaxing this assumption affects the magnitude of net supply shock effects on bond yields. Second, it would be useful to explicitly model the links with other markets, such as swap markets, especially in regard to increases in short-term interest rates. Lastly, it is important to recognize that a prerequisite for this paper's analysis is that market participants are convinced of the fiscal sustainability of the government.

Appendix A: Derivation of equation (*)

This appendix derives equation (*) in the text, i.e., the drift term of the factor dynamics under the $\mathcal{Q}$-measure, which is crucial in solving for bond prices.

Apply Ito's lemma to the pricing function ($P_t(\tau) \equiv f(\tau, \hat{r}_t, \beta_t)$) to obtain the following equation:

$$\begin{aligned} & df(\tau, \hat{r}_t, \beta_t) \\ = \; & -f_\tau(\tau, \hat{r}_t, \beta_t)dt + f_r(\tau, \hat{r}_t, \beta_t)d\hat{r}_t + f_\beta(\tau, \hat{r}_t, \beta_t)d\beta_t + \frac{1}{2}f_{rr}(\tau, \hat{r}_t, \beta_t)\langle d\hat{r}_t\rangle^2 \\ & + \frac{1}{2}f_{\beta\beta}(\tau, \hat{r}_t, \beta_t)\langle d\beta_t\rangle^2 + f_r(\tau, \hat{r}_t, \beta_t)f_\beta(\tau, \hat{r}_t, \beta_t)\langle d\hat{r}_t, d\beta_t\rangle. \end{aligned} \tag{A-1}$$

Thus, the conditional expectation of $dP_t(\tau)$ under the $\mathcal{P}$ measure can be expressed as follows.

$$\begin{aligned} & E_t^{\mathcal{P}}[dP_t(\tau)] \\ = \; & -f_\tau(\tau, \hat{r}_t, \beta_t)dt + f_r(\tau, \hat{r}_t, \beta_t)\kappa_r(\mu - \hat{r}_t)dt - f_\beta(\tau, \hat{r}_t, \beta_t)\kappa_\beta\beta_t dt \\ & + \frac{1}{2}f_{rr}(\tau, \hat{r}_t, \beta_t)\sigma_r^2 dt + \frac{1}{2}f_{\beta\beta}(\tau, \hat{r}_t, \beta_t)\sigma_\beta^2 dt + f_r(\tau, \hat{r}_t, \beta_t)f_\beta(\tau, \hat{r}_t, \beta_t)\rho\sigma_r\sigma_\beta dt. \end{aligned} \tag{A-2}$$

By the $\mathcal{Q}$-measure factor dynamics (eq, (12)), the conditional expectation of $dP_t(\tau)$ under the $\mathcal{Q}$-measure can be expressed as follows.

$$\begin{aligned} & E_t^{\mathcal{Q}}[dP_t(\tau)] \\ = \; & -f_\tau(\tau, \hat{r}_t, \beta_t)dt + f_r(\tau, \hat{r}_t, \beta_t)\mu_r^{\mathcal{Q}}(\hat{r}_t, \beta_t)dt + f_\beta(\tau, \hat{r}_t, \beta_t)\mu_\beta^{\mathcal{Q}}(\hat{r}_t, \beta_t)dt \\ & + \frac{1}{2}f_{rr}(\tau, \hat{r}_t, \beta_t)\sigma_r^2 dt + \frac{1}{2}f_{\beta\beta}(\tau, \hat{r}_t, \beta_t)\sigma_\beta^2 dt + f_r(\tau, \hat{r}_t, \beta_t)f_\beta(\tau, \hat{r}_t, \beta_t)\rho\sigma_r\sigma_\beta dt. \end{aligned} \tag{A-3}$$

Now, the first-order condition for arbitrageurs (eq. (7)) can be rewritten as follows.

$$\begin{aligned} & E_t^{\mathcal{P}}\left[\frac{dP_t(\tau)}{P_t(\tau)}\right] \\ = \; & E_t^{\mathcal{Q}}\left[\frac{dP_t(\tau)}{P_t(\tau)}\right] + a\;\; Cov_t^{\mathcal{P}}\left[\frac{dP_t(\tau)}{P_t(\tau)}, \int_0^{T^*}\left(\theta_0(s) + \alpha\big(s, P_t(s)\big)\log P_t(s) + \theta(s)\beta_t\right)\frac{dP_t(s)}{P_t(s)}ds\right], \end{aligned} \tag{A-4}$$

where by no-arbitrage condition

$$E_t^{\mathcal{Q}}\left[\frac{dP_t(\tau)}{P_t(\tau)}\right] = r_t dt. \tag{A-5}$$

Combine eqs. (A-2), (A-3), and (A-4) to obtain

$$\begin{aligned} & f_r(\tau, \hat{r}_t, \beta_t)\kappa_r(\mu - \hat{r}_t)dt - f_\beta\;(\tau, \hat{r}_t, \beta_t)\kappa_\beta\beta_t dt \\ = \; & f_r(\tau, \hat{r}_t, \beta_t)\mu_r^{\mathcal{Q}}(\hat{r}_t, \beta_t)dt + f_\beta\;(\tau, \hat{r}_t, \beta_t)\mu_\beta^{\mathcal{Q}}(\hat{r}_t, \beta_t)dt \\ & + a\;\; Cov_t^{\mathcal{P}}\left[dP_t(\tau), \int_0^{T^*}\left(\theta_0(s) + \alpha\big(s, P_t(s)\big)\log P_t(s) + \theta(s)\beta_t\right)\frac{dP_t(s)}{P_t(s)}ds\right], \end{aligned} \tag{A-6}$$

where

$$
\begin{aligned}
& Cov_t^{\mathcal{P}}\left[dP_t(\tau), \int_0^{T^*}\left(\theta_0(s)+\alpha\big(s,P_t(s)\big)\log P_t(s)+\theta(s)\beta_t\right)\frac{dP_t(s)}{P_t(s)}ds\right] \\
= & \int_0^{T^*}\left(\theta_0(s)+\alpha\big(s,P_t(s)\big)\log P_t(s)+\theta(s)\beta_t\right) cov_t^{\mathcal{P}}\left[dP_t(\tau), \frac{dP_t(s)}{P_t(s)}\right]ds \\
= & \int_0^{T^*}\left(\begin{array}{c}\dfrac{\left(\theta_0(s)+\alpha\big(s,P_t(s)\big)\log P_t(s)+\theta(s)\beta_t\right)}{P_t(s)}\times \\ \left(\begin{array}{c} f_r(\tau,\hat{r}_t,\beta_t)f_r(s,\hat{r}_t,\beta_t)\sigma_r^2dt+f_\beta(\tau,\hat{r}_t,\beta_t)f_\beta(s,\hat{r}_t,\beta_t)\sigma_\beta^2dt \\ +f_r(\tau,\hat{r}_t,\beta_t)f_\beta(s,\hat{r}_t,\beta_t)\rho\sigma_r\sigma_\beta dt+f_\beta(\tau,\hat{r}_t,\beta_t)f_r(s,\hat{r}_t,\beta_t)\rho\sigma_r\sigma_\beta dt \end{array}\right)\end{array}\right)ds.
\end{aligned}
\tag{A-7}
$$

The eq. (A-6) can be expressed in the following matrix form

$$
\begin{aligned}
& [f_r(\tau,\hat{r}_t,\beta_t) \quad f_\beta(\tau,\hat{r}_t,\beta_t)]\begin{bmatrix}\mu_r^{\mathcal{Q}}(\hat{r}_t,\beta_t)\\ \mu_\beta^{\mathcal{Q}}(\hat{r}_t,\beta_t)\end{bmatrix} \\
= & [f_r(\tau,\hat{r}_t,\beta_t) \quad f_\beta(\tau,\hat{r}_t,\beta_t)]\begin{bmatrix}\kappa_r(\mu-\hat{r}_t)\\ -\kappa_\beta\beta_t\end{bmatrix} \\
& -a[f_r(\tau,\hat{r}_t,\beta_t) \quad f_\beta(\tau,\hat{r}_t,\beta_t)]\begin{bmatrix}\sigma_r^2 & \rho\sigma_r\sigma_\beta\\ \rho\sigma_r\sigma_\beta & \sigma_\beta^2\end{bmatrix} \\
& \times\begin{bmatrix}\int_0^{T^*}\dfrac{(\theta_0(s)+\alpha(s,f(s,\hat{r}_t,\beta_t))\log f(s,\hat{r}_t,\beta_t)+\theta(s)\beta_t)}{f(s,\hat{r}_t,\beta_t)}\ f_r(s,\hat{r}_t,\beta_t)ds\\ \int_0^{T^*}\dfrac{(\theta_0(s)+\alpha(s,f(s,\hat{r}_t,\beta_t))\log f(s,\hat{r}_t,\beta_t)+\theta(s)\beta_t)}{f(s,\hat{r}_t,\beta_t)}f_\beta(s,\hat{r}_t,\beta_t)ds\end{bmatrix}.
\end{aligned}
$$

Since the above equation holds for any τ, $\hat{r}_t$, and β_t, the following drift terms are obtained.

$$
\begin{aligned}
& \begin{bmatrix}\mu_r^{\mathcal{Q}}(\hat{r}_t,\beta_t)\\ \mu_\beta^{\mathcal{Q}}(\hat{r}_t,\beta_t)\end{bmatrix} \\
= & \begin{bmatrix}\kappa_r(\mu-\hat{r}_t)\\ -\kappa_\beta\beta_t\end{bmatrix}-a\begin{bmatrix}\sigma_r^2 & \rho\sigma_r\sigma_\beta\\ \rho\sigma_r\sigma_\beta & \sigma_\beta^2\end{bmatrix} \\
& \times\begin{bmatrix}\int_0^{T^*}\dfrac{(\theta_0(s)+\alpha(s,f(s,\hat{r}_t,\beta_t))\log f(s,\hat{r}_t,\beta_t)+\theta(s)\beta_t)}{f(s,\hat{r}_t,\beta_t)}\ f_r(s,\hat{r}_t,\beta_t)ds\\ \int_0^{T^*}\dfrac{(\theta_0(s)+\alpha(s,f(s,\hat{r}_t,\beta_t))\log f(s,\hat{r}_t,\beta_t)+\theta(s)\beta_t)}{f(s,\hat{r}_t,\beta_t)}f_\beta(s,\hat{r}_t,\beta_t)ds\end{bmatrix}.
\end{aligned}
\tag{*}
$$

Appendix B: Numerical Algorithm

We conduct Monte Carlo simulations to numerically solve the model by approximating bond prices as follows.

$$
P_t(\tau)=f(\tau,\hat{r}_t,\beta_t)\approx\frac{1}{N_j}\sum_{j=1}^{N_j}\exp\left(-\sum_{i=t}^{t+N_{T^*}}r_i\,(j)h\right) \tag{B-1}
$$

where $r_i(j)$ is the model-implied period i short rate under the jth simulation path, T^* is the maximum maturity in years, N_{T^*} is the maximum maturity corresponding simulated frequency h ($N_{T^*} = T^*/h$), and N_j is the total number of simulations. We set $T^* = 20$ years, $h = 1/52$ (for weekly frequency) and $N_j = 10{,}000$. The factor dynamics under the $\mathcal{Q}$ measure are approximated as follows

$$\hat{r}_{i+1}(j) \approx \hat{r}_i(j) + \mu_r^{\mathcal{Q}}\big(\hat{r}_i(j), \beta_i(j)\big)h + \sigma_r\sqrt{h}\ \ \varepsilon_r(i;j), \tag{B-2}$$

$$\beta_{i+1}(j) \approx \beta_i(j) + \mu_\beta^{\mathcal{Q}}\big(\hat{r}_i(j), \beta_i(j)\big)h + \sigma_\beta\sqrt{h}\ \ \varepsilon_\beta(i;j). \tag{B-3}$$

The drift terms $\mu_r^{\mathcal{Q}}(\hat{r}_i(j), \beta_i(j))$ and $\mu_\beta^{\mathcal{Q}}\big(\hat{r}_i(j), \beta_i(j)\big)$ are approximated as follows,

$$\begin{aligned}
&\begin{bmatrix}\mu_r^{\mathcal{Q}}(\hat{r}_i(j), \beta_i(j))\\ \mu_\beta^{\mathcal{Q}}\big(\hat{r}_i(j), \beta_i(j)\big)\end{bmatrix}\\
\approx\ &\begin{bmatrix}\kappa_r(\mu - \hat{r}_i(j))\\ -\kappa_\beta\beta_i(j)\end{bmatrix} - a\begin{bmatrix}\sigma_r^2 & \rho\sigma_r\sigma_\beta\\ \rho\sigma_r\sigma_\beta & \sigma_\beta^2\end{bmatrix}\\
&\times\sum_{l=1}^{N_l}\begin{bmatrix}w_l\Big(\theta_0(s_l) + \alpha\Big(s_l, f\big(s_l, \hat{r}_i(j), \beta_i(j)\big)\Big)\log f\big(s_l, \hat{r}_i(j), \beta_i(j)\big) + \theta(s_l)\beta_i(j)\Big)\\ \times\dfrac{f_r\big(s_l, \hat{r}_i(j), \beta_i(j)\big)}{f\big(s_l, \hat{r}_i(j), \beta_i(j)\big)}\\ w_l\Big(\theta_0(s_l) + \alpha\Big(s_l, f\big(s_l, \hat{r}_i(j), \beta_i(j)\big)\Big)\log f\big(s_l, \hat{r}_i(j), \beta_i(j)\big) + \theta(s_l)\beta_i(j)\Big)\\ \times\dfrac{f_\beta\big(s_l, \hat{r}_i(j), \beta_i(j)\big)}{f\big(s_l, \hat{r}_i(j), \beta_i(j)\big)}\end{bmatrix},
\end{aligned} \tag{B-4}$$

where ρ represents the correlation coefficient between $\varepsilon_r(i;j)$ and $\varepsilon_\beta(i;j)$ and w_l is weight for sparse grid integration based on Heiss and Winschel (2008).

Numerical algorithm to solve VV-ELB when $\alpha = 0$

The VV-ELB with $\alpha = 0$ is numerically solved by applying a few approximations. First, we linearly approximate the drift term (eq. (*)) around the neighborhood of $(r_t, \beta_t) = \big(\mu_r^*, \mu_\beta^*\big)$. The factor dynamics under the $\mathcal{Q}$ measure can be simplified as follows.

$$\begin{bmatrix}dr_t\\ d\beta_t\end{bmatrix} = \kappa^*\begin{bmatrix}\mu_r^* - r_t\\ \mu_\beta^* - \beta_t\end{bmatrix}dt + \begin{bmatrix}\sigma_r dB_{r,t}\\ \sigma_\beta dB_{\beta,t}\end{bmatrix} \tag{B-5}$$

where κ^*, μ_r^*, and μ_β^* satisfy

$$\begin{aligned}
\mu_r^{\mathcal{Q}}(r_t, \beta_t) \approx\ & \mu_r^{\mathcal{Q}}\big(\mu_r^*, \mu_\beta^*\big) + \frac{\partial\mu_r^{\mathcal{Q}}}{\partial r}\big(\mu_r^*, \mu_\beta^*\big)(r_t - \mu_r^*) + \frac{\partial\mu_r^{\mathcal{Q}}}{\partial\beta}\big(\mu_r^*, \mu_\beta^*\big)\big(\beta_t - \mu_\beta^*\big), \qquad \text{(B-6)}\\
=\ & \kappa_{11}^*\mu_r^* + \kappa_{12}^*\mu_\beta^* - \kappa_{11}^* r_t - \kappa_{12}^*\beta_t,\\
\mu_\beta^{\mathcal{Q}}(r_t, \beta_t) \approx\ & \mu_\beta^{\mathcal{Q}}\big(\mu_r^*, \mu_\beta^*\big) + \frac{\partial\mu_\beta^{\mathcal{Q}}}{\partial r}\big(\mu_r^*, \mu_\beta^*\big)(r_t - \mu_r^*) + \frac{\partial\mu_\beta^{\mathcal{Q}}}{\partial\beta}\big(\mu_r^*, \mu_\beta^*\big)\big(\beta_t - \mu_\beta^*\big), \qquad \text{(B-7)}
\end{aligned}$$

$$= \kappa_{21}^{*}\mu_r^{*} + \kappa_{22}^{*}\mu_\beta^{*} - \kappa_{21}^{*}r_t - \kappa_{22}^{*}\beta_t,$$

thus the following equations hold,

$$\mu_r^{\mathcal{Q}}(\mu_r^{*},\mu_\beta^{*}) - \frac{\partial \mu_r^{\mathcal{Q}}}{\partial r}(\mu_r^{*},\mu_\beta^{*})\mu_r^{*} - \frac{\partial \mu_r^{\mathcal{Q}}}{\partial \beta}(\mu_r^{*},\mu_\beta^{*})\mu_\beta^{*} = \kappa_{11}^{*}\mu_r^{*} + \kappa_{12}^{*}\mu_\beta^{*}, \tag{B-8}$$

$$-\frac{\partial \mu_r^{\mathcal{Q}}}{\partial r}(\mu_r^{*},\mu_\beta^{*}) = \kappa_{11}^{*}, \tag{B-9}$$

$$-\frac{\partial \mu_r^{\mathcal{Q}}}{\partial \beta}(\mu_r^{*},\mu_\beta^{*}) = \kappa_{12}^{*}, \tag{B-10}$$

$$\mu_\beta^{\mathcal{Q}}(\mu_r^{*},\mu_\beta^{*}) - \frac{\partial \mu_\beta^{\mathcal{Q}}}{\partial r}(\mu_r^{*},\mu_\beta^{*})\mu_r^{*} - \frac{\partial \mu_\beta^{\mathcal{Q}}}{\partial \beta}(\mu_r^{*},\mu_\beta^{*})\mu_\beta^{*} = \kappa_{21}^{*}\mu_r^{*} + \kappa_{22}^{*}\mu_\beta^{*}, \tag{B-11}$$

$$-\frac{\partial \mu_\beta^{\mathcal{Q}}}{\partial r}(\mu_r^{*},\mu_\beta^{*}) = \kappa_{21}^{*}, \tag{B-12}$$

$$-\frac{\partial \mu_\beta^{\mathcal{Q}}}{\partial \beta}(\mu_r^{*},\mu_\beta^{*}) = \kappa_{22}^{*}. \tag{B-13}$$

Second, following Priebsch (2013) and Ueno (2017), we apply a second-order approximation to the government bond pricing function as follows,

$$P_t(\tau) = f(\tau, r_t, \beta_t) \approx \exp\left(-E_t^{\mathcal{Q}}\left[\int_t^T \max(r_u, b)\, du\right] + \frac{1}{2} Var_t^{\mathcal{Q}}\left[\int_t^T \max(r_u, b)\, du\right]\right). \tag{B-14}$$

The drift terms under the $\mathcal{Q}$ measure can be expressed as follows,

$$\mu_r^{\mathcal{Q}}(\mu_r^{*},\mu_\beta^{*})$$

$$= \kappa_r(\mu - \mu_r^{*}) - a\begin{bmatrix}\sigma_r^2 & \rho\sigma_r\sigma_\beta\end{bmatrix}\begin{bmatrix}\int_0^{T^{*}} \frac{(\theta_0(s) + \theta(s)\mu_\beta^{*}) f_r(s,\mu_r^{*},\mu_\beta^{*})}{f(s,\mu_r^{*},\mu_\beta^{*})}\, ds \\ \int_0^{T^{*}} \frac{(\theta_0(s) + \theta(s)\mu_\beta^{*}) f_\beta(s,\mu_r^{*},\mu_\beta^{*})}{f(s,\mu_r^{*},\mu_\beta^{*})}\, ds\end{bmatrix},$$

$$= \kappa_r(\mu - \mu_r^{*})$$

$$-a\int_0^{T^{*}} \left[\sigma_r^2 \frac{\partial}{\partial r} + \rho\sigma_r\sigma_\beta \frac{\partial}{\partial \beta}\right]\left\{\begin{array}{l} -E_t^{\mathcal{Q}}\left[\int_t^{t+s} \max(r_u, b)\, du\right] \\ +\frac{1}{2} Var_t^{\mathcal{Q}}\left[\int_t^{t+s} \max(r_u, b)\, du\right]\end{array}\right\} \Bigg|_{r=\mu_r^{*},\beta=\mu_\beta^{*}} (\theta_0(s) + \theta(s)\mu_\beta^{*}) \times ds,$$

$$\mu_\beta^{\mathcal{Q}}(\mu_r^{*},\mu_\beta^{*})$$

$$= -\kappa_\beta \mu_\beta^* - a\begin{bmatrix}\rho\sigma_r\sigma_\beta & \sigma_\beta^2\end{bmatrix}\begin{bmatrix}\int_0^{T^*} \frac{(\theta_0(s)+\theta(s)\mu_\beta^*) f_r(s,\mu_r^*,\mu_\beta^*)}{f(s,\mu_r^*,\mu_\beta^*)}\, ds \\ \int_0^{T^*} \frac{(\theta_0(s)+\theta(s)\mu_\beta^*) f_\beta(s,\mu_r^*,\mu_\beta^*)}{f(s,\mu_r^*,\mu_\beta^*)}\, ds\end{bmatrix}$$

$$= -\kappa_\beta \mu_\beta^* - a\int_0^{T^*}\left[\rho\sigma_r\sigma_\beta\frac{\partial}{\partial r}+\sigma_\beta^2\frac{\partial}{\partial\beta}\right]\left\{\begin{array}{c}(\theta_0(s)+\theta(s)\mu_\beta^*)\times \\ -E_t^Q\left[\int_t^{t+s}\max(r_u,b)\,du\right] \\ +\frac{1}{2}Var_t^Q\left[\int_t^{t+s}\max(r_u,b)\,du\right]\end{array}\right\}\Bigg|_{r=\mu_r^*,\beta=\mu_\beta^*} ds.$$

The derivatives of the drift terms with respect to each factor can be expressed as follows,

$$\frac{\partial \mu_r^Q}{\partial r}(\mu_r^*,\mu_\beta^*)ds \tag{B-15}$$

$$= -\kappa_r - a\int_0^{T^*}\left[\sigma_r^2\frac{\partial^2}{\partial r^2}+\rho\sigma_r\sigma_\beta\frac{\partial^2}{\partial r\partial\beta}\right]\left\{\begin{array}{c}(\theta_0(s)+\theta(s)\mu_\beta^*)\times \\ -E_t^Q\left[\int_t^{t+s}\max(r_u,b)\,du\right] \\ +\frac{1}{2}Var_t^Q\left[\int_t^{t+s}\max(r_u,b)\,du\right]\end{array}\right\}\Bigg|_{r=\mu_r^*,\beta=\mu_\beta^*} ds,$$

$$\frac{\partial \mu_\beta^Q}{\partial r}(\mu_r^*,\mu_\beta^*) \tag{B-16}$$

$$= -a\int_0^{T^*}\left[\rho\sigma_r\sigma_\beta\frac{\partial^2}{\partial r^2}+\sigma_\beta^2\frac{\partial^2}{\partial r\partial\beta}\right]\left\{\begin{array}{c}(\theta_0(s)+\theta(s)\mu_\beta^*)\times \\ -E_t^Q\left[\int_t^{t+s}\max(r_u,b)\,du\right] \\ +\frac{1}{2}Var_t^Q\left[\int_t^{t+s}\max(r_u,b)\,du\right]\end{array}\right\}\Bigg|_{r=\mu_r^*,\beta=\mu_\beta^*} ds,$$

$$\frac{\partial \mu_r^Q}{\partial \beta}(\mu_r^*,\mu_\beta^*) \tag{B-17}$$

$$= -a\int_0^{T^*}\left[\sigma_r^2\frac{\partial}{\partial r}+\rho\sigma_r\sigma_\beta\frac{\partial}{\partial\beta}\right]\left\{\begin{array}{c}\theta(s)\times \\ -E_t^Q\left[\int_t^{t+s}\max(r_u,b)\,du\right] \\ +\frac{1}{2}Var_t^Q\left[\int_t^{t+s}\max(r_u,b)\,du\right]\end{array}\right\}\Bigg|_{r=\mu_r^*,\beta=\mu_\beta^*} ds,$$

$$\frac{\partial \mu_\beta^Q}{\partial \beta}(\mu_r^*, \mu_\beta^*) \tag{B-18}$$

$$= -\kappa_\beta - a\int_0^{T^*} \left\{ \left[\rho\sigma_r\sigma_\beta \frac{\partial^2}{\partial r \partial \beta} + \sigma_\beta^2 \frac{\partial^2}{\partial \beta^2}\right] \left\{ \begin{array}{c} (\theta_0(s) + \theta(s)\mu_\beta^*) \times \\ -E_t^Q\left[\int_t^{t+s} \max(r_u, b)\, du\right] \\ +\frac{1}{2} Var_t^Q\left[\int_t^{t+s} \max(r_u, b)\, du\right] \end{array} \right\} \Bigg|_{r=\mu_r^*, \beta=\mu_\beta^*} \right\} ds$$

$$-a\int_0^{T^*} \left\{ \left[\rho\sigma_r\sigma_\beta \frac{\partial}{\partial r} + \sigma_\beta^2 \frac{\partial}{\partial \beta}\right] \left\{ \begin{array}{c} \theta(s) \times \\ -E_t^Q\left[\int_t^{t+s} \max(r_u, b)\, du\right] \\ +\frac{1}{2} Var_t^Q\left[\int_t^{t+s} \max(r_u, b)\, du\right] \end{array} \right\} \Bigg|_{r=\mu_r^*, \beta=\mu_\beta^*} \right\} ds.$$

We numerically solve $(\kappa^*,\ \mu_r^*,\ \mu_\beta^*)$ that satisfy equations (B-8)-(B-13) and (B-15)-(B-18) employing a numerical algorithm based on Genz (2004) for the bivariate normal distribution function and a sparse grid integration technique by Heiss and Winschel (2008).

Numerical algorithm to solve VV-Alpha

To solve VV-Alpha, we set the targeted maturity (τ^*) at 10 years and the cap (y^*) at 0.25 percent to be consistent with the Japanese YCC. In order to obtain the initial bond prices, we discretize the state and maturity space and solve VV for the case of $\alpha = 0$. Given these bond prices, we then introduce the α-function (eq. (10)) for different values of α and solve for bond prices for each considered value of α by iterating until they converge via a Monte Carlo simulation and cubic spline interpolation (Dierckx, 1993).

Appendix C: Data description

The maturity structure data

We use the maturity structure database of Japanese government bonds constructed by Koeda and Kimura (2022). Their database compiles the bond issue level information for the end of each fiscal year since 1965 using data from the BOJ, Japan Securities Dealers Association, and the Ministry of Finance, Japan. Using this database, we compute the bonds outstanding by maturity as a fraction of GDP, netting out the BOJ holdings and their estimated private preferred habitat bond holdings, in order to construct the maturity structure variables used in the calibration. Specifically, the first PCA component on the maturity structure variables with remaining maturity 1-20 years corresponds to Figure 2 in the text. The data sample used in the calibration is 1995-2014.

The survey data on TIBOR

The survey data consists of predictions for 3-month TIBOR by the Consensus Forecast which are available from 2017 at quarterly frequency. The surveys are taken at the very start of each quarter and thus, as in Wright (2011), the timing convention that we adopt is to treat the survey for any given quarter as referring to forecasts at the end of the previous quarter. Given the data limitation, we use the data from January 2017-October 2021. To mitigate constraints arising from an ELB on nominal interest rates, we only use over 4-year ahead predictions.

Bond yield data

Bloomberg zero coupon bond yields are available from April 1989. The data sample is the end of fiscal years 1995-2014 for 3-month and 1, 2, 5 10, 20-year maturities.

Appendix D: Calibration using an extended Kalman filter

Parameters (ρ and a) are estimated via pseudo-likelihood function maximization using an extended Kalman filter with the observation equation approximated by

$$\boldsymbol{y_t} = \boldsymbol{f}(\hat{r}_t, \beta_t) + \boldsymbol{w_t},$$

where

$$\begin{aligned}\boldsymbol{f}(\hat{r}_t, \beta_t) &\approx \boldsymbol{f}\big(\hat{E}[\hat{r}_t|\beta_t, \mathcal{F}_{t-1}], \beta_t\big) + \frac{\partial \boldsymbol{f}}{\partial r}\big(\hat{E}[\hat{r}_t|\beta_t, \mathcal{F}_{t-1}], \beta_t\big)\big(\hat{r}_t - \hat{E}[\hat{r}_t|\beta_t, \mathcal{F}_{t-1}]\big) \\ &\equiv \boldsymbol{A_0}\big(\hat{E}[\hat{r}_t|\beta_t, \mathcal{F}_{t-1}], \beta_t\big) + \boldsymbol{A_r}\big(\hat{E}[\hat{r}_t|\beta_t, \mathcal{F}_{t-1}], \beta_t\big)\hat{r}_t,\end{aligned}$$

and $\boldsymbol{y_t}$ is a vector of bond yields with different maturities, $\boldsymbol{w_t}$ is a vector of i.i.d measurement errors allowing for different variances for each element. The state equations are given by

$$\begin{bmatrix} d\hat{r}_t \\ d\beta_t \end{bmatrix} = \kappa \begin{bmatrix} \mu - \hat{r}_t \\ -\beta_t \end{bmatrix} dt + \begin{bmatrix} \sigma_r dB_{r,t} \\ \sigma_\beta dB_{\beta,t} \end{bmatrix}, \ \kappa \equiv \begin{bmatrix} \kappa_r & 0 \\ 0 & \kappa_\beta \end{bmatrix}.$$

We treat $\hat{r}_t$ as a latent variable and β_t as an observed variable. $\hat{E}[\hat{r}_t|\beta_t, \mathcal{F}_{t-1}]$ is a linear projection of $\hat{r}_t$ on β_t and information set in period $t-1$ ($\mathcal{F}_{t-1}$). We assume $\hat{E}[\hat{r}_1|\beta_1, \mathcal{F}_0] = \hat{E}[\hat{r}_1|\mathcal{F}_0] + \Sigma_{12}\Sigma_{22}^{-1}\big(\beta_1 - \hat{E}[\beta_1|\mathcal{F}_0]\big) = \mu + \Sigma_{12}\Sigma_{22}^{-1}\beta_1$ and $P_{r,1|0} = \sigma_r^2/(2\kappa_r)$ and use the following equation to predict and update,

$$\hat{E}[\hat{r}_{t+1}|\beta_{t+1}, \mathcal{F}_t] = \hat{E}[\hat{r}_{t+1}|\mathcal{F}_t] + \Sigma_{12}\Sigma_{22}^{-1}(\beta_{t+1} - e^{-\kappa_\beta}\beta_t),$$

where

$$\begin{aligned}&\hat{E}[\hat{r}_{t+1}|\mathcal{F}_t] \\ =\ & (1 - e^{-\kappa_r})\mu + e^{-\kappa_r}\hat{E}[\hat{r}_t|\mathcal{F}_{t-1}] + e^{-\kappa_r}\Sigma_{12}\Sigma_{22}^{-1}e^{-\kappa_\beta t}\int_{t-1}^{t} e^{\kappa_\beta s}\,\sigma_\beta dB_{\beta,s} \\ &+ e^{-\kappa_r}\big[P_{r,t|t-1} - \Sigma_{12}\Sigma_{22}^{-1\top}\Sigma_{12}^{\top}\big]A_r\big(\hat{E}[\hat{r}_t|\beta_t, \mathcal{F}_{t-1}], \beta_t\big)^{\top}\end{aligned}$$

$$\times \begin{bmatrix} A_r\left(\hat{E}[\hat{r}_t|\beta_t,\mathcal{F}_{t-1}],\beta_t\right)P_{r,t|t-1}A_r\left(\hat{E}[\hat{r}_t|\beta_t,\mathcal{F}_{t-1}],\beta_t\right)^{\top} \\ -A_r\left(\hat{E}[\hat{r}_t|\beta_t,\mathcal{F}_{t-1}],\beta_t\right)\Sigma_{12}\Sigma_{22}^{-1\top}\Sigma_{12}^{\top}A_r\left(\hat{E}[\hat{r}_t|\beta_t,\mathcal{F}_{t-1}],\beta_t\right)^{\top}+R \end{bmatrix}^{-1}$$

$$\times \begin{pmatrix} y_t - A_0\left(\hat{E}[\hat{r}_t|\beta_t,\mathcal{F}_{t-1}],\beta_t\right) - A_r\left(\hat{E}[\hat{r}_t|\beta_t,\mathcal{F}_{t-1}],\beta_t\right)\hat{E}[\hat{r}_t|\mathcal{F}_{t-1}] \\ -A_r\left(\hat{E}[\hat{r}_t|\beta_t,\mathcal{F}_{t-1}],\beta_t\right)\Sigma_{12}\Sigma_{22}^{-1}e^{-\kappa_\beta t}\int_{t-1}^{t} e^{\kappa_\beta s}\,\sigma_\beta dB_{\beta,s} \end{pmatrix},$$

and

$$\begin{aligned} & P_{r,t+1|t} \\ = \; & e^{-\kappa_r}\left(P_{r,t|t-1}-\Sigma_{12}\Sigma_{22}^{-1\top}\Sigma_{12}^{\top}\right)e^{-\kappa_r^{\top}} \\ & -e^{-\kappa_r}\left(P_{r,t|t-1}-\Sigma_{12}\Sigma_{22}^{-1\top}\Sigma_{12}^{\top}\right)A_r\left(\hat{E}[\hat{r}_t|\beta_t,\mathcal{F}_{t-1}],\beta_t\right)^{\top} \\ & \times\left[A_r\left(\hat{E}[\hat{r}_t|\beta_t,\mathcal{F}_{t-1}],\beta_t\right)\left(P_{r,t|t-1}-\Sigma_{12}\Sigma_{22}^{-1\top}\Sigma_{12}^{\top}\right)A_r\left(\hat{E}[\hat{r}_t|\beta_t,\mathcal{F}_{t-1}],\beta_t\right)^{\top}+R\right]^{-1} \\ & \times A_r\left(\hat{E}[\hat{r}_t|\beta_t,\mathcal{F}_{t-1}],\beta_t\right)\left(P_{r,t|t-1}-\Sigma_{12}\Sigma_{22}^{-1\top}\Sigma_{12}^{\top}\right)^{\top}e^{-\kappa_r^{\top}}+\Sigma_{11}. \end{aligned}$$

The estimated parameters and the standard deviations of measurement error are listed as follows.

ρ	-0.2852
a	15.067
3M	0.0012
1Y	0.0008
2Y	0.0012
5Y	0.0041
10Y	0.0065
20Y	0.0075

References

Bank of Japan, "Comprehensive Assessment of the Monetary Easing (the Background)," September 21, 2016.

――, "Assessment for Further Effective and Sustainable Monetary Easing (the Background)," March 19, 2021.

――, "Statement on Monetary Policy," April 28, 2022.

Bernanke, Ben, "The Latest from the Bank of Japan," Brookings Institution Ben Bernanke's Blog, September 21, 2016.

Carlson, Mark, Stefania D'Amico, Cristina Fuentes-Albero, Bernd Schlusche, and Paul Wood, "Issues in the Use of the Balance Sheet Tool," Finance and Economics Discussion Series 2020-070, Federal Reserve Board, 2020.

Chaurushiya, Radha, and Ken Kuttner, "Targeting the Yield Curve: The Experience of the Federal Reserve, 1942-1951," memorandum to the Federal Open Market Committee, Board of Governors of the Federal Reserve System, Division of Research and Statistics, June 18, 2003, https://www.federalreserve.gov/monetarypolicy/2003-fomc-memos.htm.

D'Amico, Stefania, and Thomas King, "Flow and Stock Effects of Large-Scale Treasury Purchases : Evidence on the Importance of Local Supply," *Journal of Financial Economics*, 108(2), 2013, pp.425–448.

Dierckx, Paul, *Curve and Surface Fitting with Splines*, Oxford University Press, 1993.

Federal Reserve Board, "Minutes of the Federal Open Market Committee June 9–10, 2020," July 1, 2020.

Fukunaga, Ichiro, Naoya Kato, and Junko Koeda, "Maturity Structure and Supply Factors in Japanese Government Bond Markets," *Monetary and Economic Studies*, 33, Institute for Monetary and Economic Studies, Bank of Japan, 2015, pp.45-96.

Genz, Alan, "Numerical Computation of Rectangular Bivariate and Trivariate Normal and t Probabilities," *Statistics and Computing,* 14, 2004, pp. 251–260.

Grande, Giuseppe, Adriana Grasso, and Gabriele Zinna, "The Effectiveness of the ECB's Asset Purchases at the Lower Bound," Questioni di Economia e Finanza (Occasional Papers), 2019.

Hamilton, James and Jing Cynthia Wu, "The Effectiveness of Alternative Monetary Policy Tools in a Zero Lower Bound Environment," *Journal of Money, Credit and Banking*, 44 (s1), 2012, pp. 3-46.

Harvey, Andrew, *Forecasting, Structural Time Series Models and the Kalman Filter*, Cambridge University Press, 1989.

Hattori, Takahiro and Yoshida, Jiro, "Yield Curve Control," 2021 (available at SSRN:

https://ssrn.com/abstract=3396251).

Heiss, Florian, and Viktor Winschel, "Likelihood Approximation by Numerical Integration on Sparse Grids," *Journal of Econometrics*, 14(1), May 2008, pp. 62–80.

Higgins, Matthew and Thomas Klitgaard, "Japan's Experience with Yield Curve Control," Federal Reserve Bank of New York Liberty Street Economics, June 22, 2020, https://libertystreeteconomics.newyorkfed.org/2020/06/japans-experience-with-yield-curve-control.html.

Ito, Takayasu, "Short-Term Cross-Currency Basis Swap and Japanese Government Bond Markets under Non-Traditional Monetary Policy," *Asia-Pacific Contemporary Finance and Development* (*International Symposia in Economic Theory and Econometrics*, 26), Emerald Publishing Limited, Bingley, 2019, pp. 27-39.

Keynes, John, *The General Theory of Employment, Interest, and Money*, London: Macmillan, 1936.

King, Thomas, "Expectation and Duration at the Effective Lower Bound," *Journal of Financial Economics*, 134(3), 2019, pp.736–760.

Koeda, Junko, and Yosuke Kimura, "Government Debt Maturity and the Term Structure in Japan," 2022 (available at SSRN: https://papers.ssrn.com/sol3/papers.cfm?abstract_id=4015576).

Kuroda, Haruhiko, "'Quantitative and Qualitative Monetary Easing with Yield Curve Control': After Half a Year since Its Introduction", Speech at a Reuters Newsmaker Event in Tokyo, 2017.

――, "Outlook for Economic Activity and Prices and Monetary Policy," Speech at a Meeting Held by the Naigai Josei Chosa Kai (Research Institute of Japan), 2021a.

――, "Monetary Policy and Firms' Behavior: Transmission Channels of Monetary Policy and Japanese Firms' Structural Changes," Speech at the Meeting of Councillors of Nippon Keidanren (Japan Business Federation) in Tokyo, 2021b.

Lucca, David and Jonathan Wright, "The Narrow Channel of Quantitative Easing: Evidence from YCC Down Under," Federal Reserve Bank of New York Staff Reports, No. 1013, 2022.

Priebsch, Marcel, "Computing Arbitrage-Free Yields in Multi-Factor Gaussian Shadow-Rate Term Structure Models," Finance and Economics Discussion Series 2013-63, Federal Reserve Board, 2013.

Reserve Bank of Australia, "Minutes of the Monetary Policy Meeting of the Reserve Bank Board," November 2, 2021.

Sudo, Nao and Masaki Tanaka, "Quantifying Stock and Flow Effects of QE," *Journal of Money, Credit and Banking*, 53(7), 2021, pp. 1719-1755.

Tobin, James, "A General Equilibrium Approach to Monetary Theory, " *Journal of Money, Credit and Banking*, 1(1), 1969, pp. 15-29.

Ueno, Yoichi, "Term Structure Models with Negative Interest Rates," Bank of Japan IMES Discussion Paper No. 2017-E-1, Institute for Monetary and Economic Studies, Bank of Japan, 2017.

Vayanos, Dimitri, and Jean-Luc Vila, "A Preferred-Habitat Model of the Term Structure of Interest Rates," *Econometrica*, 89(1), 2021, pp. 77–112.

Wallace, Neil, "A Modigliani-Miller Theorem for Open-Market Operations," *American Economic Review* 71(3), 1981, pp. 267–274.

Wright, Jonathan, "Term Premia and Inflation Uncertainty: Empirical Evidence from an International Panel Dataset," *American Economic Review*, 101(4), 2011, pp.1514-1534.